

Amorphous superconducting lanthanum-gold alloys obtained by liquid quenching*

W. L. Johnson, S. J. Poon, and P. Duwez

W. M. Keck Laboratory of Engineering Materials, California Institute of Technology, Pasadena, California 91109

(Received 14 March 1974; revised manuscript received 1 July 1974)

Results of x-ray diffraction, electrical resistivity, and critical magnetic field measurements are presented for amorphous superconducting lanthanum-gold alloys obtained by liquid quenching. The transition temperature of the alloys is $\sim 3.5^\circ\text{K}$. The bulk nature of the samples along with the stability of the amorphous phase at room temperature make this an ideal system for the study of superconductivity in the amorphous state. Estimates of intrinsic parameters including the coherence length ξ and penetration depth λ are presented and discussed. The observed linearity of $H_{c2}(T)$ and its extrapolated low-temperature limiting value are discussed and compared to predicted behavior for $H_{c2}(T)$.

I. INTRODUCTION

A growing body of literature exists on the subject of superconductivity in highly disordered and amorphous materials. To date, however, experimental reports of superconductivity in amorphous materials all concern thin films obtained by vapor deposition on a cryogenic substrate. Amorphous phases thus obtained anneal into crystalline states at rather low temperatures. For example, amorphous bismuth films with a superconducting transition temperature $T_c = 6^\circ\text{K}$ (Ref. 1) are found to crystallize above 20°K .^{2,3} Furthermore, the amorphous phase can only be obtained for films with thickness less than about 600 \AA .⁴ Amorphous gallium films with $T_c = 8.4^\circ\text{K}$ (Ref. 5) anneal into crystalline βGa above 15°K .^{6,7} Superconductivity in "amorphous" transition-metal alloy films has also been reported.⁸ However, the electron diffraction patterns (containing three to four diffuse rings) used to characterize the structure of these films are consistent with the existence of a highly disordered microcrystalline structure. Unfortunately, the effects of low density, microcrystallinity, gaseous contamination, and large internal surface area may all play a significant role in the superconductivity of thin films. Thus results for thin films may not be comparable to those obtained for a bulk metallic glass the density of which is close to that of the corresponding crystalline phase.

In this paper, we report the results of x-ray diffraction analysis, electrical resistivity measurements, and critical magnetic field measurements for bulk amorphous superconducting La-Au alloys obtained by liquid quenching. Based on these experimental results, estimates of several intrinsic parameters characteristic of the superconducting state are presented and discussed in conjunction with the observed behavior of $H_{c2}(T)$, the upper critical field. Samples used in this work are in the form of foils having an area of about 1 to 2 cm^2 and a uniform thickness of about $60 \text{ }\mu\text{m}$. Regarding the stability of the amorphous phase, it should

be noted that no crystallization is observed at room temperature during periods of several weeks.

II. EXPERIMENTAL PROCEDURES

Alloys of the form $\text{Au}_x\text{La}_{100-x}$ were studied with $0 \leq x \leq 40$. For $16 \leq x \leq 30$, alloys were investigated at intervals of every 2 at.%. In addition, several alloys of Cu-La and Ni-La were studied and an amorphous superconducting phase was obtained in these systems. Most of the results reported are for Au-La alloys. Alloys were prepared by induction melting of the appropriate constituents on a silver boat under an argon atmosphere. Samples were then quenched from the liquid state using both the "gun" and the "piston and anvil" techniques described in Ref. 9. The cooling rate from the liquid state is estimated to be of the order $10^6^\circ\text{C}/\text{sec}$.

The structure of each sample was checked by x-ray scanning with a Norelco diffractometer (Cu $K\alpha$ radiation). Lattice parameters of the associated crystalline phases were obtained from Debye-Scherrer films using the Nelson-Riley extrapolation function. Electrical resistivity as a function of temperature was measured using a standard four-probe technique. The temperature was determined using a germanium resistance thermometer with an accuracy of $\pm 0.02^\circ\text{K}$. Critical magnetic field (H_{c2}) measurements were performed using a superconducting solenoid for magnetic fields up to 40 kG oriented transversely to the sample and temperatures down to 1.85°K . The temperature for H_{c2} measurements was determined by measuring the vapor pressure over the liquid- He^4 bath.

III. RESULTS

A. Structure analysis

An approximate nonequilibrium phase diagram illustrating the compositional range of phases present in liquid-quenched $\text{Au}_x\text{La}_{100-x}$ alloys is shown in Fig. 1. This diagram is based on the results of x-ray diffraction analysis. For $0 \leq x \leq 14$, a crys-

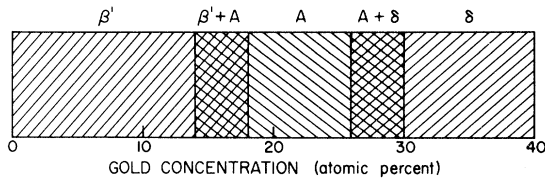


FIG. 1. Phases present in liquid quenched La-Au alloys as a function of gold concentration (at. %). The fcc solid solution is designated as β' , the amorphous phase as A , and the new cubic crystalline phase as δ .

talline phase (designated as β') is obtained having the fcc structure of β -La with Au in solid solution. In the range $14 \lesssim x \lesssim 18$, liquid-quenched alloys contain both the β' phase and an amorphous phase. For alloys with $18 \lesssim x \lesssim 26$, a single amorphous phase can be obtained. For $26 \lesssim x \lesssim 30$, alloys contain both the amorphous phase and a new cubic crystalline phase the structure of which has not been determined. No amorphous phase was observed for $x \geq 30$.

The x-ray diffraction intensity as a function of scattering angle (2θ) for the alloy $\text{Au}_{22}\text{La}_{78}$ containing a single amorphous phase is shown in Fig. 2. The pattern shows a broad maximum centered at 30.7° with a full width at half-maximum of 4.8° . According to the Scherrer formula, this corresponds to an effective microcrystal size of 17 \AA , which is typical of a glassy metal. It has been shown that although only α -La (hcp) is stable at room temperature, β -La (fcc) can be retained by rapid quenching.¹⁰ On the basis of the anomalously large coefficient of diffusion for Au in β -La, it has been suggested that impurity Au atoms occupy the octahedral interstitial voids in the fcc unit cell.¹¹⁻¹³ In view of these facts, it is probable that the structure of the β' phase resembles that of β -La with Au atoms occupying interstitial voids in solid solu-

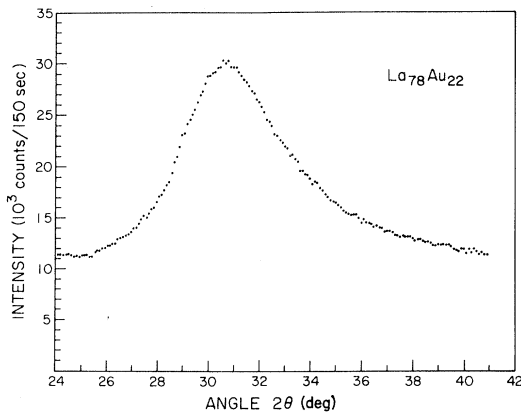


FIG. 2. X-ray diffraction intensity as a function of scanning angle (2θ) for amorphous $\text{Au}_{22}\text{La}_{78}$.

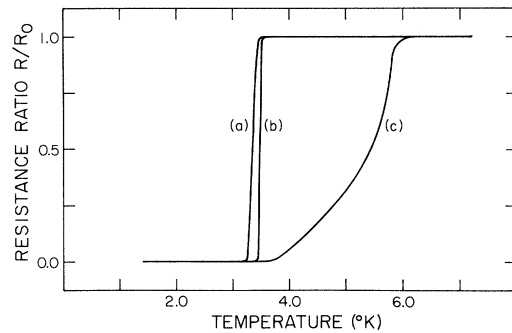


FIG. 3. Resistance ratio R/R_0 as a function of temperature for (a) amorphous $\text{Au}_{22}\text{La}_{78}$ obtained using the "gun" technique, (b) amorphous $\text{Au}_{22}\text{La}_{78}$ obtained using the "piston and anvil" technique with $\rho_0 = 3.0 \times 10^{-4} \Omega \text{ cm}$, (c) liquid-quenched La containing the β phase obtained using the "gun" technique.

tion. Assuming that the single amorphous phase should be formed when each unit cell of β -La contains an average of one interstitially dissolved Au atom gives an estimated composition of $\text{Au}_{20}\text{La}_{80}$ for the single amorphous phase consistent with the observed composition range and the Bernal model for random-packed structures.¹⁴ Although no significant annealing effect is observed at room temperature during periods of several weeks, it was found that annealing at 100°C for several hours results in the onset of crystallization. Spontaneous crystallization is observed at temperatures of about 150 to 200°C .

B. Electrical resistivity

Results of electrical resistivity measurements as a function of temperature for two $\text{Au}_{22}\text{La}_{78}$ samples and liquid-quenched lanthanum containing β -La are shown in Fig. 3. A sharp resistive transition (transition width $\approx 0.1^\circ\text{K}$) with $T_c = 3.4^\circ\text{K}$, indicative of a single phase, is observed for the amorphous $\text{Au}_{22}\text{La}_{78}$ samples. For liquid-quenched lanthanum, a much broader transition with an onset temperature of 6.0°K (T_c of β -La) is observed. Resistivity measurements for single-phase amorphous samples ($18 \lesssim x \lesssim 26$) gives a temperature coefficient of resistivity $[1/\rho_0(T)][d\rho(T)/dT]$ of order $10^{-4}^\circ\text{K}^{-1}$ and a residual resistivity ρ_0 in the range 2×10^{-4} to $4 \times 10^{-4} \Omega \text{ cm}$ at 10°K , characteristic of a glassy metal. Critical current density (J_c) measurements give $J_c \sim 10^4 \text{ A/cm}^2$ at a temperature of 1.5°K .

To illustrate the dependence of T_c on alloy composition, a plot is shown in Fig. 4. In the figure, vertical bars are used to indicate the transition widths. It can be seen that alloys containing a crystalline phase have rather broad [transition width $\approx (1-2)^\circ\text{K}$] transitions. For alloys containing less than 18-at. % Au, the onset temperature

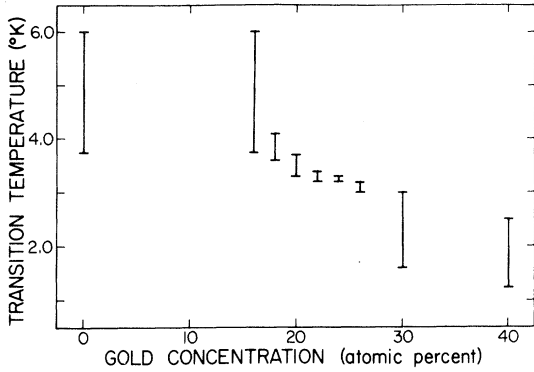


FIG. 4. Superconducting transition temperature as a function of alloy composition. Vertical bars indicate the width of the transitions.

for superconductivity (T_c') is about 6°K; this can presumably be identified as the transition temperature of crystalline β -La. Alloys containing more than 26-at. % Au have a broad transition which is complete only below 2°K. This lower transition temperature may be associated with the new unidentified cubic crystalline phase previously mentioned. To compare this new crystalline phase with the equilibrium AuLa_2 phase, an as cast sample of $\text{Au}_{33}\text{La}_{67}$ was annealed at 600°C for one week. A sharp superconducting transition with $T_c = 3.2^\circ\text{K}$ was observed indicating that the new crystalline phase obtained in liquid-quenched samples is not identical to the equilibrium structure.

The superconducting transition temperatures of amorphous $\text{Cu}_{30}\text{La}_{70}$ and $\text{La}_{78}\text{Ni}_{22}$ were determined from electrical resistivity to be 3.5°K and 3.0°K, respectively. The residual resistivity, temperature coefficient of resistivity, and superconducting transition width are all comparable to those observed for amorphous Au-La alloys.

C. Critical field (H_{c2}) measurements

Results of H_{c2} measurements obtained in a superconducting solenoid for both amorphous and highly disordered crystalline $\text{Au}_{24}\text{La}_{76}$ samples are shown in Fig. 5. The crystalline sample, with an x-ray diffraction pattern exhibiting several peaks, was obtained by liquid quenching at a cooling rate insufficient to yield an amorphous phase. This sample, however, remains highly disordered as evidenced by a residual resistivity $\rho_0 \approx 3 \times 10^{-4} \Omega \text{ cm}$ comparable to that of the amorphous sample. To define H_{c2} in this measurement, the magnetic field (transverse to the sample foil) was increased at a constant temperature until a measurable nonzero resistivity ($\sim 10^{-3}\rho_0$) was observed for the sample. For the amorphous sample, $H_{c2}(T)$ is observed to be linear throughout the temperature range investigated. The behavior of $H_{c2}(T)$ for the highly dis-

ordered crystalline sample is rather different from that of the amorphous sample. A lower value of $H_{c2}(T)$ is obtained for $T < 2.6^\circ\text{K}$, and significant departure from linearity can be seen. It should be mentioned that the transition from the superconducting state to the normal state was completely reversible. Values for $H_{c2}(T)$ obtained by decreasing H with $H > H_{c2}(T)$ initially are to within an experimental error of $\sim 50 \text{ G}$, identical to those obtained by increasing H with $H < H_{c2}(T)$ initially.

IV. DISCUSSION

To gain some insight into the intrinsic properties of the amorphous superconducting alloys, the following calculations are presented. In the "dirty limit," the coherence length of a superconductor near T_c is given by¹⁵

$$\xi(t) = 0.85 (\xi_0 l)^{1/2} (1-t)^{-1/2}, \quad (1)$$

where $t = T/T_c$ (the reduced temperature), l is the electronic mean free path in the normal state, and $\xi_0 = \hbar v_F / \pi \Delta$ (the coherence length for a clean material at $t=0$). In the weak-coupling limit,¹⁶ the energy gap is given by $\Delta = 1.75 k_B T_c$. The coherence length can also be approximated by¹⁷

$$\xi(t) = [\Phi_0 / 2\pi H_{c2}(t)]^{1/2}, \quad (2)$$

where Φ_0 is the fundamental flux quantum. Using the linear dependence of $H_{c2}(t)$ observed for $0.5 \leq t \leq 1$ (Fig. 5) for amorphous $\text{Au}_{24}\text{La}_{76}$ and Eq. (2) gives

$$\xi(t) = 1.13 \times 10^{-6} (1-t)^{-1/2} \quad (3)$$

over the measured temperature range. This can be compared to Eq. (1) by estimating the product $\xi_0 l$ using the free-electron model for the amor-

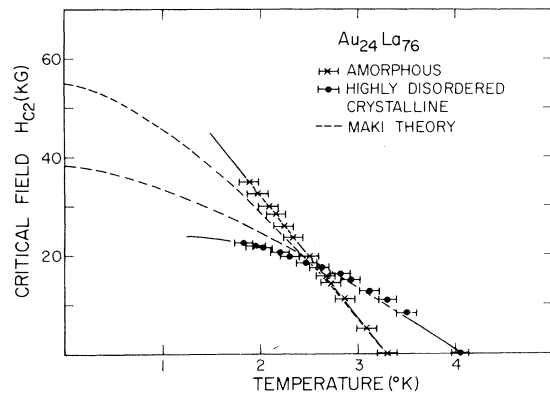


FIG. 5. Upper critical field as a function of temperature for amorphous ($T_c = 3.3^\circ\text{K}$) and highly disordered crystalline ($T_c = 4.0^\circ\text{K}$) $\text{Au}_{24}\text{La}_{76}$ alloys. Dashed lines are obtained using the Maki expression given in Eq. (6).

phous alloy. Experimental values of $N(0)$, the electronic density of states at the Fermi level, for β -La have been deduced from specific heat and magnetic susceptibility measurements, both giving $N(0) \approx 1.9$ states/eV atom.^{18,19} Using a valence of three for β -La in the free-electron model gives 2.2 states/eV atom, in close agreement with experiment. The electronic mean collision time is extremely small in the amorphous phase and thus no rapid variation of $N(E)$ is expected. The free-electron model can be used as a reasonable first approximation to the electronic properties of the amorphous phase. The effect of Au is ignored and the values $N(0) \approx 2.2$ states/eV atom and $v_F \approx 1.6 \times 10^8$ cm/sec are used. From the measured value of $\rho_0 \approx 3 \times 10^{-4}$ Ω cm for the residual resistivity, the electronic mean free path is estimated to be 1.9 Å. Taking the observed $T_c = 3.3^\circ\text{K}$ and using the weak-coupling limit gives $\xi_0 \approx 6.2 \times 10^{-5}$ cm. Equation (1) then reduces to

$$\xi(t) \approx 0.92 \times 10^{-8} (1-t)^{-1/2}. \quad (4)$$

This can be compared to Eq. (3), which is derived from Eq. (2). The agreement is reasonable.

In the dirty limit, the penetration depth is given by¹⁷

$$\lambda(t) = 0.615 \lambda_L(0) (\xi_0/l)^{1/2} (1-t)^{-1/2}, \quad (5)$$

where $\lambda_L(0)$ is the London penetration depth. Thus κ , the Ginzburg-Landau parameter, can be estimated. Using Eq. (4) for $\xi(t)$ and Eq. (5) for $\lambda(t)$ gives $\kappa \approx 70$. Summarizing, type-II behavior characterized by an extremely large Ginzburg-Landau parameter is observed.

For a severely disordered crystal lattice, in particular for an amorphous material where the electronic mean free path is the order of the interatomic distance, an extremely large upper critical field H_{c2} is expected. Gor'kov²⁰ estimated the maximum critical field attainable for a given T_c to be $H_{c2}^{\text{max}} \approx 10^4 T_c$ G. By considering the paramagnetic contribution to the free energy of the normal state, Clogston²¹ derived the expression $H_{c2}^{\text{max}} \approx 1.8 \times 10^4 T_c$ G. Maki²² and Werthamer *et al.*²³ have extended the Abrikosov-Gorkov formalism to all temperatures and have included the paramagnetic effect pointed out by Clogston and the effect of spin-orbit scattering on the behavior of $H_{c2}(t)$ in the dirty limit $l \ll \xi_0$. Maki²⁴ and DeGennes²⁵ show that by ignoring the paramagnetic and spin-orbit effects in the dirty limit $H_{c2}(t)$ can be related to t throughout the range $0 < t < 1$ by

$$\ln(1/t) = \psi(1 + eDH_{c2}/2\pi ck_B T_c t) - \psi(\frac{1}{2}), \quad (6)$$

where $D = \frac{1}{3} v_F l$ is the diffusivity and ψ is the digamma function. This expression reduces to

$$H_{c2}(t) = \frac{4k_B T_c}{\pi e} (c/D) (1-t) \left[1 - \left(\frac{1}{2} - \frac{28}{\pi^4} \zeta(3) (1-t) \right) \right] \quad (7a)$$

for $t \rightarrow 1$ and

$$H_{c2}(t) = 0.87 (c/D) (k_B T_c / e) \left[1 - \frac{2}{3} \left(\frac{\pi t}{1.75} \right)^2 \right] \quad (7b)$$

for $t \rightarrow 0$.

Equations (7) were used to fit the observed $H_{c2}(t)$ curves of Fig. 5. The parameter D was determined by requiring agreement between the observed values of $H_{c2}(t)$ and those predicted by Eq. (7a) for $t \leq 1$. For amorphous $\text{Au}_{24}\text{La}_{76}$, a value of $D \approx 0.454$ cm^2/sec is obtained; for the highly disordered crystalline sample $D \approx 0.671$ cm^2/sec . The low-temperature limiting behavior of $H_{c2}(t)$ for each case is then determined by inserting these values of D in Eq. (7b). This gives $H_{c2}(t=0) \approx 55$ kG for the amorphous sample and $H_{c2}(t=0) \approx 37$ kG for the highly disordered crystalline sample. The value of D for the amorphous sample can be compared to the value $D = \frac{1}{3} v_F l = 1.00$ cm^2/sec calculated from the free-electron model as in Eq. (4). The discrepancy is probably related to the errors introduced by the free-electron approximation.

It is seen in Fig. 5 that the exact shape of the observed $H_{c2}(t)$ curves deviates from the shape predicted by Eq. (6). For the amorphous sample, the observed linearity of $H_{c2}(T)$ extends to lower temperatures than predicted by Eq. (6). For the disordered crystalline sample, Eq. (6) predicts larger values than observed for $H_{c2}(T)$ below $T \approx 2.5^\circ\text{K}$. Equation (6) has been extended by Werthamer and co-workers^{23,26} to include both the paramagnetic effect and the effect of spin-orbit scattering. The paramagnetic effect tends to suppress $H_{c2}(T)$ at low temperatures and probably accounts for the lower values of $H_{c2}(T)$ observed for the disordered crystalline sample below $T \approx 2.5^\circ\text{K}$ as compared to values predicted by Eq. (6). The spin-orbit scattering effect, however, tends to compensate for the paramagnetic suppression and tends to restore the linearity of $H_{c2}(T)$. The linearity of $H_{c2}(T)$ over a large temperature range observed for highly disordered thin films has been explained by the presence of a large spin-orbit scattering effect.²⁷ The same argument can be applied to the present amorphous sample. It is interesting that the spin-orbit scattering effect is apparently much stronger in the amorphous sample than in the highly disordered crystalline sample.

Several additional experiments will provide useful information for understanding the fundamental properties of the amorphous Au-La system. First, it would be interesting to measure the energy gap directly from tunneling or infrared absorption experiments. Tunneling and infrared absorption experiments suggest that lanthanum is a weakcoupling

superconductor.^{28,29} It has been suggested that amorphous superconductors tend to be strong coupling.³⁰ It would also be interesting to obtain the phonon spectrum of amorphous Au-La alloys. A measurement of the low-temperature specific heat would provide experimental values $N(0)$ and Θ_D (Debye temperature). The value of $N(0)$ is essential for understanding the electronic structure of the amorphous alloys.

On the basis of the present work, several comments can be made regarding the theory of superconductivity applied to amorphous materials. First, it has been observed that amorphous Au-La, Cu-La, and Ni-La alloys have nearly the same T_c . Second, since the electronic mean free path in all of these alloys is of the order of interatomic distances, it is clear that the electronic interactions which lead to pairing must be of a local nature. These two facts taken together indicate that the bonding char-

acteristics of La-La nearest neighbors determine the superconducting properties of these alloys. It would be interesting to attempt to prepare bulk amorphous superconducting alloys of the 4d and 5d transition-metal series. It has been suggested that bonding involving d orbitals plays an essential role in the superconductivity of these metals.³¹ The study of amorphous transition-metal alloys would help to isolate the role played by the bonding of d electrons from that played by large variations in the density of states at the Fermi surface and variations in crystal structure. Such an investigation is currently underway in this laboratory.

ACKNOWLEDGMENT

The authors wish to thank Wilkie Y. K. Chen for designing the superconducting solenoid used for the upper critical field measurements.

*Work supported by the U. S. Atomic Energy Commission.

¹W. Buckel and R. Hilsch, *Z. Phys.* **138**, 109 (1954).

²N. Barth, *Z. Phys.* **142**, 58 (1955).

³W. Buckel and R. Hilsch, *Z. Phys.* **146**, 27 (1956).

⁴B. G. Lazarev, V. M. Kuz'menko, A. I. Sudovtsov, and V. M. Mil'nikov, *Dokl. Akad. Nauk SSSR* **194**, 302 (1970) [*Sov. Phys.—Dokl.* **15**, 846 (1971)].

⁵W. Buckel and R. Hilsch, *Z. Phys.* **138**, 118 (1954).

⁶W. Buckel, *Z. Phys.* **138**, 136 (1954).

⁷Satauri Fujime, *Jpn. J. Appl. Phys.* **5**, 764 (1966).

⁸M. M. Collver and R. H. Hammond, *Phys. Rev. Lett.* **30**, 92 (1973).

⁹P. Duwez, *Progress in Solid State Chemistry* (Pergamon, Oxford and New York, 1966).

¹⁰M. J. Marcinkowski and E. N. Hopkins, *Trans. AIME (Am. Inst. Min. Metall. Pet. Eng.)* **242**, 579 (1968).

¹¹M. P. Daniel, G. Erez, and G. M. J. Schmidt, *Philos. Mag.* **19**, 1053 (1969).

¹²T. R. Anthony and D. Turnbull, *Phys. Rev.* **151**, 495 (1966).

¹³T. R. Anthony and D. Turnbull, *Appl. Phys. Lett.* **8**, 120 (1966).

¹⁴J. D. Bernal, *Proc. R. Soc. A* **280**, 299 (1964).

¹⁵P. G. De Gennes, *Superconductivity of Metals and Alloys* (Benjamin, New York, 1966).

¹⁶J. Bardeen, L. Cooper, and J. Schrieffer, *Phys. Rev.*

108, 1175 (1957).

¹⁷D. Saint-James, G. Sarma, and E. J. Thomas, *Theory of Type II Superconductivity* (Pergamon, Oxford, 1969).

¹⁸K. Andres, *Phys. Rev.* **168**, 708 (1968).

¹⁹D. Wohlleben, thesis (University of California, La Jolla, 1968) (unpublished).

²⁰L. P. Gor'kov, *Zh. Eksp. Teor. Fiz.* **37**, 833 (1960) [*Sov. Phys.—JETP* **10**, 593 (1960)].

²¹A. M. Clogston, *Phys. Rev. Lett.* **9**, 266 (1962).

²²K. Maki, *Phys. Rev.* **148**, 362 (1966).

²³N. R. Werthamer, E. Helfand, and P. C. Hohenberg, *Phys. Rev.* **147**, 295 (1966).

²⁴K. Maki, *Physics (N. Y.)* **1**, 127 (1964).

²⁵P. G. De Gennes, *Phys. Kondens. Mater.* **3**, 79 (1964).

²⁶E. Helfand and N. R. Werthamer, *Phys.* **147**, 288 (1966).

²⁷M. Ashkin, D. W. Deis, J. R. Gavaler, and C. K. Jones, *AIP Conf. Proc.* **4**, 204 (1972).

²⁸J. D. Leslie, R. L. Cappelletti, D. M. Ginsberg, D. K. Finnemore, F. H. Spedding, and B. J. Beaudry, *Phys. Rev.* **134**, A 309 (1964).

²⁹J. J. Hauser, *Phys. Rev. Lett.* **17**, 921 (1966).

³⁰J. E. Jackson, C. V. Briscoe, and H. Wühl, *Physica (Utr.)* **55**, 447 (1971).

³¹D. M. Gualtieri, *J. Appl. Phys.* **45**, 1880 (1974).